www.czasopisma.pan.pl PAN www.journals.pan.pl
POLSKA AKADEMIA NAUK

Metrol. Meas. Syst., Vol. 23 (2016), No. 4, pp. 531–543.

PAN POLSKA AKADEMIA NAUK

METROLOGY AND MEASUREMENT SYSTEMS

Index 330930, ISSN 0860-8229

www.metrology.pg.gda.pl

M&MS

CURRENT FLUCTUATION MEASUREMENTS OF AMPEROMETRIC GAS SENSORS CONSTRUCTED WITH THREE DIFFERENT TECHNOLOGY PROCEDURES

Petr Sedlak[1)], Petr Kubersky[2)], Pavel Skarvada[1)], Ales Hamacek[2)], Vlasta Sedlakova[1)], Jiri Majzner[1)], Stanislav Nespurek [2)], Josef Sikula[1)]

1) Brno University of Technology, Faculty of Electrical Engineering and Communications, Technicka 8, Brno 616 00, Czech Republic (✉ sedlakp@feec.vutbr.cz, +420 54 114 3208, skarvada@feec.vutbr.cz, sedlaka@feec.vutbr.cz, jiri.majzner@ceitec.vutbr.cz, Josef.Sikula@ceitec.vutbr.cz)

2) University of West Bohemia, Faculty of Electrical Engineering, Plzen 306 14, Czech Republic (kubersky@ket.zcu.cz, hamacek@ket.zcu.cz, nespurek@post.cz)

Abstract

Electrochemical amperometric gas sensors represent a well-established and versatile type of devices with unique features: good sensitivity and stability, short response/recovery times, and low power consumption. These sensors operate at room temperature, and therefore have been applied in monitoring air pollutants and detection of toxic and hazardous gases in a number of areas . Some drawbacks of classical electrochemical sensors are overcome by the *solid polymer electrolyte* (SPE) based on ionic liquids. This work presents evaluation of an SPE-based amperometric sensor from the point of view of current fluctuations. The sensor is based on a novel three-electrode sensor platform with solid polymer electrolytes containing ionic liquid for detection of nitrogen dioxide – a highly toxic gas that is harmful to the environment and presenting a possible threat to human health even at low concentrations. The paper focuses on using noise measurement (electric current fluctuation measurement) for evaluation of electrochemical sensors which were constructed by different fabrication processes: (i) lift-off and drop-casting technology, (ii) screen printing technology on a ceramic substrate and (iii) screen printing on a flexible substrate.

Keywords: current fluctuations, noise measurement, amperometric sensor, solid polymer electrolyte.

1. Introduction

Gas detection plays crucial role in a wide spectrum of applications, such as security, medicine, food technology, environmental protection, *etc*. Various chemical and physical principles are employed for quantitative measurement of specific gases [1, 2]. Among various approaches, electrochemical principles show advantages over other techniques. As a part of a large and important class [3], the electrochemical amperometric gas sensors provide high sensitivity at low cost, and are versatile devices with good stability, short response/recovery time and low power consumption [4–6]. Moreover, they operate at room temperature which is required in many applications.

Classical electrochemical sensors contain liquid acidic electrolytes. This fact may cause several disadvantages: (i) there is a danger of leakage of acidic electrolyte, (ii) a considerable size of sensors make their integration into smart sensor systems inconvenient, (iii) sensor construction is not suitable for low-cost mass production techniques, (iv) problems arise from evaporation of the internal electrolyte [7]. As a remedy, *solid polymer electrolyte* (SPE) can be used [3, 4, 7–10]. SPE is based on organic ionic liquid held up in a polymer matrix. *Ionic liquids* (ILs) represent low-temperature molten salts with their melting points below 100ºC, and are usually composed of organic cations and inorganic/organic anions. The salts are combinations

Article history: received on Dec. 22, 2015; accepted on May 05, 2016; available online on Dec. 12, 2016; DOI: 10.1515/mms-2016-0042.

of a large cation and a charge-delocalized anion, thus are typically characterized by weak interactions. This fact results in a low tendency to crystallize due to flexibility (anion) and dissymmetry (cation). ILs may undergo almost unlimited structural variations because of the easy preparation of a large variety of their components. A number of salts can be used to design the ionic liquid that has the required properties for a given application. Thus, ILs are currently widely used in various fields of electrochemistry and chemistry because of their unique properties, such as non-flammability, non-volatility, wide electrochemical windows, excellent thermal and electrochemical stability, relatively high conductivity, *etc*. Due to those properties, ionic liquids are attractive materials for use in electrochemical sensors [4, 5, 10, 11]. Application of ILs in electrochemical sensors has a potential to broaden or even revolutionize the range of analytical methods [12, 13].

Transport of electrical charge at active interfaces of sensor is tightly linked with the principles of electrochemical sensors and their properties (detection capability, selectivity, dynamic response, *etc*.). Understanding the sensor behaviour requires a description of these phenomena. Besides standard techniques (such as DC electrical conductivity measurement, AC electrical impedance measurement, *etc*.) supplementary information can be obtained using noise spectroscopy, since several authors proved that low-frequency current fluctuations are associated with conductive mechanisms [14]. Moreover, the noise spectroscopy give us integral information about the complete state of a device and may inform about faults in its design, quality of electrical contacts and conducting paths, applied manufacturing processes, long-term stability, etc. An increased level of noise or unusual shape of the noise spectra usually indicate failure mechanisms in particular devices [14–18]. Several authors showed that fluctuation analysis enables to extract a more selective response from the chemical sensors, [19–24], surface acoustic wave sensors, and resonant sensors [25, 26].

2. Amperometric gas sensors

Amperometry is a conventional electroanalytical technique that is widely applied wherever it is necessary to identify and quantify the electroactive species in the liquid or gaseous phase. The first two subsections present a brief general description of the principle and design of amperometric sensors. The third subsection deals with fabrication of sensors.

2.1. Principle of operation

A typical electrochemical sensor is designed according to the principles used in electrochemical cells with two or three electrodes, as shown in Fig. 1. A fundamental two-electrode sensor consists of a working (sensing) electrode, a counter electrode and an ionically conductive phase (electrolyte/buffer), which provides transport of charge within the sensor and links all electrodes [3]. When a proper potential is kept between the electrodes, electroactive species in electrolyte participate in electrochemical reactions, such as oxidation or reduction, on the surfaces of particular electrodes. The *working electrode* (WE) reacts with the detected matter, while the counter electrode acts conversely to balance the charges added or removed from the electrolyte by redox reactions at WE, when the amperometric cell is connected to an external circuit in which electrons flow [2]. Thus, the current (electron) flow is generated as a function of the detected matter's concentration. In other words, the exact number of electrons are generated per each molecule of detected matter. Then, the charge is exactly related to the number of "detected" molecules reacting in the system and the electrical current is related to the rate of electrochemical reactions [3].

Addition of the third electrode to the two-electrode topology brings better stability of the sensor response. The third electrode, called a *reference electrode* (RE), serves as the true

Metrol. Meas. Syst., Vol. 23 (2016), No. 4, pp. 531–543.

potential reference for WE and no current flows between WE and RE [27, 28]. With such an architecture, CE is still free to polarize without affecting WE. The amperometric sensor keeps constant sensitivity and good linearity of response to a target substance.

The detection process consists of several steps including adsorption of the analyte onto the surface, electro-reaction, and desorption of products from the electrode surface [3]. The current flowing through the sensor during exposure to the target matter can be limited either by the rate of electrode reaction (kinetic limit) or by diffusion of the reactant onto the electrode surface (diffusion limit) [3]. The electrical current in sensor depends on many factors, such as gas concentration, electric potential, and area of the working electrode [9].

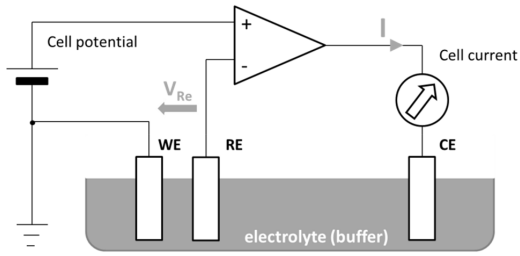

Fig. 1. A conceptual scheme of a three-electrode amperometric electrochemical cell and a potentiostat. In WE-grounded configuration: WE is kept at the ground potential, the operational amplifier controls the current flow through the cell in order to keep the required value of voltage V_{Re}.

2.2. Structure and geometry

There exist several three-electrode topologies (planar [7, 8, 29] and bulk [2, 3]). have The interface of a typical gas sensor at WE facilitates transport of gas molecules to the working electrode/electrolyte interface by simple diffusion or with an aid of a simple air pump [3]. The porous and gas-permeable membranes can be used to control the gas flow into the sensor and can aid selectivity, allowing only the analyte molecules to pass. The membrane can be made of a polymeric or organic material such as *Polytetrafluoroethylene* (PTFE) or cellulose. The electrolyte provides transport of charge within the sensor, links all electrodes, solubilizes the reactants and products for efficient transport, and is chemically and physically stable in all conditions of sensor operation [3]. Among commonly used electrolytes, solid polymer electrolytes have been given an increased attention for their unique properties [10, 11].

The electron-transfer reaction at the working electrodes involves several steps, as mentioned above. Thus, WE is typically made of a noble metal (platinum or gold). These metals generally exhibit excellent stability at a polarized potential, which may cause corrosion of other metals. Moreover, they can create a defined electrode/electrolyte interface and are sufficiently porous to allow effective diffusion of gas molecules to the large and reactive electrode/electrolyte interface. Graphite and glassy carbon are other popular choices for the working electrode.

2.3. Fabrication processes of our amperometric NO_2 sensors

The objects of our study are amperometric gas sensors based on a semi-planar three-electrode topology which consists of a working electrode, a *pseudo-reference electrode* (RE), and a *counter electrode* (CE). Fig. 2a shows the topology of sensors and examples of a laboratory sample, a sample on a ceramic substrate and a fully printed sensor. Each type was constructed in a different way.

The laboratory samples were made on a ceramic substrate (9 mm × 7 mm × 1 mm). Platinum electrodes (the pseudo-reference (2b) and counter (3b) electrodes, see Fig. 1) were constructed

by means of the "lift-off" technology. A *solid polymer electrolyte* (SPE) was applied with a glass rod onto the surface of alumina substrate and spread over both platinum electrodes. The solid polymer electrolyte consists of ionic liquid C_2mim NTf_2, a *poly(vinylidene fluoride)* (PVDF) matrix and 1-methyl-2-pyrrolidone (1:1:3 weight). Thereafter, the carbon working electrode was constructed by "drop-casting" a mixture consisting of spherical glassy carbon powder and chloroform [30]. These sensors are referred to as "laboratory samples".

The second type of samples, which is based on a ceramic substrate with platinum counter (CE) and pseudo-reference (RE) electrodes, was customized in TESLA Blatná Company (Czech Republic). The sensor element was properly sonicated in a cleaning bath and subsequently thoroughly washed in deionized water. Thereafter, a layer of *solid polymer electrolyte* (SPE) consisting of 1-ethyl-3-methylimidazolium bis(trifluoromethylsulfonyl) imide, poly(vinylidene fluoride), 1-methyl-2-pyrrolidone, and dimethylformamide (1:1:1:5, weight) was deposited with the screen printing technique. After the drying process (24 hours at 298 K), the working electrode was printed using graphite ink for screen printing (C10903P14, Gwent Group)[6]. These sensors are referred to as "ceramics Pt/SPE/C".

The fully printed sensors were constructed on a flexible poly(ethylene terephthalate) (PET) substrate (Melinex ST504, DuPont, thickness 175 μm). Their fabrication consisted of three steps [26]: printing the pseudo-reference (2b) and counter (3b) electrodes (graphite ink), printing the SPE layer, and printing the carbon working electrode. The area of fully printed sensor presented in this paper is 10 × 12 mm^2. The solid polymer electrolyte consists of ionic liquid 1-ethyl-3-methylimidazolium bis(trifluoromethylsulfonyl)imide C_2mim NTf_2, *poly(vinylidene fluoride) (PVDF)*, 1-methyl-2-pyrrolidone (NMP), and other additives, such as *dimethylformamide* (DMF) and *dimethyl sulfoxide* (DMSO), which tailored the viscosity of polymer electrolyte to the screen printing process [31]. This type of sensors is referred to as "PET C/SPE/C".

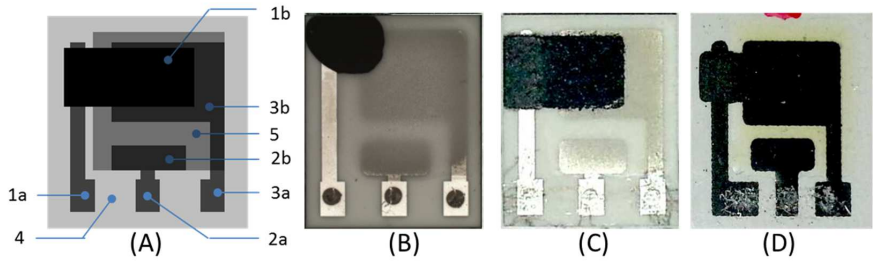

Fig. 2. a) The sensor topology: (1a) the working electrode contact; (1b) the carbon working electrode; (2a) the pseudo-reference electrode contact; (2b) the pseudo-reference electrode; 3a) the counter electrode contact; (3b) the counter electrode; 4) the substrate; 5) *the solid polymer electrolyte* (SPE); b) a laboratory sample on a ceramic substrate; c) a Pt/SPE/C sensor on a ceramic substrate; d) a fully printed sensor on PET based on graphite paste.

2.4. Morphology of active sensor interface

The morphology, geometry and structure of the working electrode and/or the interface between the *working electrode* and *solid polymer electrolyte* (WE/SPE) have a strong impact on sensor characteristics (sensitivity, response time, hysteresis, *etc.*). This fact is particularly relevant when the WE/SPE active interface is directly exposed to the detected matter, like in the case of sensors presented in this study. Moreover, in contrast to classical sensors with liquid electrolytes, it has been demonstrated that morphologies of both WE and SPE can be optimized in order to improve sensor sensitivity [8, 32]. Thus, a combination of various technological

Metrol. Meas. Syst., Vol. 23 (2016), No. 4, pp. 531–543.

approaches together with different materials can result in a unique electrochemical active interface that can be tailored to a particular detected matter.

Figure 3 presents SEM pictures of planar WE/SPE interfaces of three different samples presented in this study. The interface of a laboratory sample (Fig. 3a) consists of the layer of glassy carbon spherical particles 2–12 um (WE in Fig. 3a) and larger spherical objects whose size, clusters or deformation can be influenced by crystallization conditions during preparation of the SPE layer [32]. Although this interface provides good electrochemical activity, the structure of WE layer is vulnerable to cracks and defects which may result in bad long-term stability of the sensor response.

The interface of the second type, *i.e.*, Pt/SPE/C sensor (Fig. 3b), consists of the layer of commercial graphite ink (C10903P14, WE in Fig. 3b) and spherical objects of the SPE layer. Both layers (WE and SPE) were created with screen printing. The morphology of WE layer is given by the intrinsic properties of graphite ink and by the setup of printing process. The difference in the SPE layer morphology (lower porosity with smaller spherical objects) can be attributed to the presence of additives in forming SPE which are necessary for the screen printing process. This type of interface, prepared with the well-established printing process, exhibits lower vulnerability to defects during the use of sensor but usually shows lower electrochemical activity.

The interface of a fully printed sensor, *i.e.*, C/SPE/C sensor (Fig. 3c), consists of the layer of commercial graphite ink (C10903P14, WE in Fig. 3c) and the SPE layer. It can be seen that the morphology of SPE layer was significantly modified in order to fabricate a complete sensor with the screen printing process on a flexible PET substrate. Although this interface seems to be the worst from the point of view of electrochemical activity (a low porosity of the SPE layer and thus a low surface-to-volume ratio), sensor sensitivity can be improved by larger active areas of the electrodes (WE and CE, see Section 2.3). This procedure enables to produce an active interface with low vulnerability to defects and a sufficient response at the expense of increased sensor dimensions.

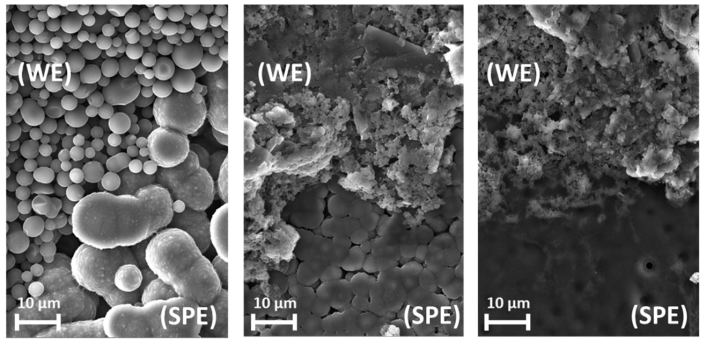

Fig. 3. SEM pictures of the planar working electrode / solid polymer electrolyte interface: a) a laboratory sample on a ceramic substrate; b) a Pt/SPE/C sensor on a ceramic substrate; c) A fully printed sensor on PET.

3. Noise in electrochemical sensors

In chemical sensors, current or voltage fluctuations are associated with physical and chemical processes which take place in the sensor structure or at its contacts (intrinsic sources) and in/on a sensing layer, or – in the case of amperometric sensor – at the electrode/electrolyte interface. The inherent noise sources are associated with conductive mechanisms in electronic devices. Thus, the fluctuations originate in amperometric sensors at the electrode/electrolyte

interface where thermal agitation, diffusion and electrochemical reactions of mobile ions take place [33, 34]. Only the thermal noise anticipates no current flow through the amperometric cell. When transfer of charge takes place at the electrode/electrolyte interface, a current-dependent fluctuation becomes apparent in addition to the thermal noise. Thus, the shape and level of spectrum are given by the charge transfer and mass transfer processes of the electro-active species, in proximity of the interface.

Exposure of a sensor to targeted substances causes appearing additional external noise sources, which come from the chemical environment, and are supposed to have a similar feature as in conductometric sensors published in the literature [20]: (i) the adsorption-desorption process of gas molecules on the active layer, (ii) diffusion of the adsorbed molecules or molecule fragments on the sensor surface. The measured spectral density of current or voltage fluctuations is assumed to result from the superposition of contributions of these two noise sources as well as the inherent noise sources.

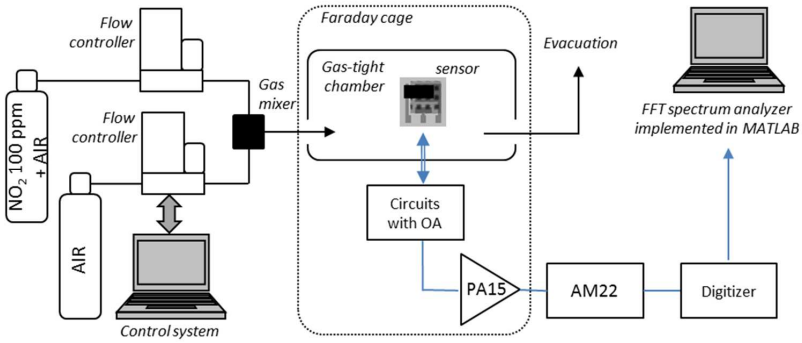

Fig. 4. An experimental apparatus designed for the study of sensor parameters.

4. Experimental setup

Figure 4 illustrates an experimental apparatus used in the study. PC-controlled mass flow controllers set flows from two gas tanks to obtain the required NO_2 concentration in a PTFE test chamber. The first gas tank was filled with a reference mixture of gaseous nitrogen dioxide and synthetic air [100 ppm NO_2], while the second one was filled only with synthetic air subsequently humidified to 40% RH.

A low-noise preamplifier PA15 (3S Sedlak, s.r.o.), an amplifier with highly selective filters AM22 (3S Sedlak, s.r.o.), a 12-bit AD convertor HS3 (TiePie engineering), and a notebook constituted a noise measurement setup. The devices as well as the measurement circuit were fed from batteries to minimize power peaks from the electrical power grid. The test chamber with an amperometric sensor and a preamplifier were located in a simple Faraday cage.

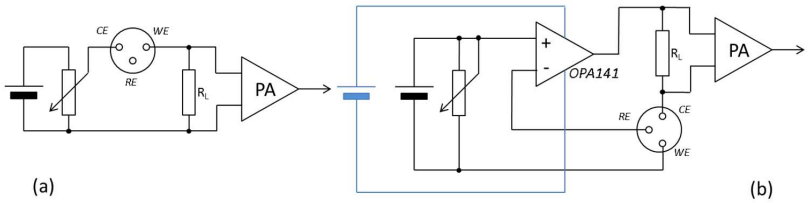

Fig. 5. A scheme of the measurement circuit for testing sensor sensitivity parameters.
a) A potentiostat controlled by an operator [6]; b) A potentiostat controlled by an operational amplifier [31].

Metrol. Meas. Syst., Vol. 23 (2016), No. 4, pp. 531–543.

The correct noise measurement is tightly linked with using a suitable apparatus and mainly with the measurement circuit of a measured sensor. Poor work conditions, such as the choice of inappropriate sensor working point (V_{RE}), lead to unreliable results. In other words, the noise measurement quality depends on the used measurement circuit of sensor and its biasing.

4.1. Measurement circuit

Several approaches to the measurement circuitry scheme were made in our study of current fluctuations in an amperometric sensor in either a neutral (zero NO_2 concentrations) or chemical (non-zero NO_2 concentrations) environment [6, 30, 31]. Generally, an amperometric sensor is the core component of a potentiostat circuit [27, 35, 36], which provides two main functions [27]: (i) controlling the voltage between the working and reference electrodes, and (ii) measuring the current flowing through the sensor, i.e. between the working and counter electrodes. Several different circuit topologies of potentiostat exist [27, 35, 36]. The measurement circuitry of potentiostat in the cooperating laboratory gave only preliminary estimation of current fluctuations, but the used apparatus presented a high level of engineering.

The measurement concept, successful in examination of noise of MOSFET [37], was carried out on the laboratory samples. The approach identified possible imperfections in particular laboratory samples [30], but it failed to measure current fluctuations when samples sensed a non-zero NO_2 concentration. Since a particular sensor is meant to be the part of potentiostat circuit based on an operation amplifier, we focused only on the simplest version of potentiostat based on the grounded WE configuration [27]. To minimize noise generated by other electronic components and to exclude influence of the operational amplifier, the measurement circuit consisted only of a battery, a potentiometer, a sensor and a loading resistance [6]. Fig. 5a presents a scheme of the circuit. The human operator sets the voltage between CE and WE of the sensor by potentiometer assuring a constant potential difference between RE and WE ($V_{RE} = 0.5$ V) to emulate the operation mode [8] for each NO_2 concentration. Current fluctuations of a particular sensor were determined by measurement of voltage fluctuations across the loading resistor. This time-consuming technique revealed an influence of higher NO_2 concentration on the power spectra of current fluctuations, It is the technique of measuring – at a minimal background noise level – the amperometric sensor fabricated by the cooperating laboratory [6].

The next solution examining current fluctuations is a potentiostat circuit based on a rail-to-rail operational amplifier (such as OPA2344 or OPA141 – Texas Instruments), in the grounded WE configuration. The measurement circuit still contains a loading resistor, a potentiometer and batteries as the power sources, as shown in Fig. 5b. The non-inverting input of the operation amplifier is held at a voltage level adjusted by the potentiometer ($V = 0.5$ V) and the operational amplifier controls the current flowing through the sensor to keep the potential between RE and WE at its required value ($V_{RE} = 0.5$ V). As in the previous case, the current fluctuations are determined by measuring the voltage fluctuations across the loading resistor.

The experimental results of two last approaches bring almost the same shape and level of noise spectral densities in the same samples. We assume that the additional noise introduced by the rail-to-rail operational amplifier is negligible compared with the current fluctuations of our sensors. Thus, the third measurement circuit seems to be the best choice for studying current fluctuations in an amperometric sensor.

5. Results and discussion

The experimental study of current fluctuations was carried out on three technologically different amperometric sensors. The sensors were exposed to a range of NO_2 concentrations

from 0 ppm up to 10 ppm except for ceramic Pt/SPE/C samples, which were limited by 3 ppm due to the stability requirements. We focused on comparison of samples from the points of view of shape and level of spectral density of current fluctuations, dependence of noise spectral densities on NO_2 concentration and signal-to-noise ratios.

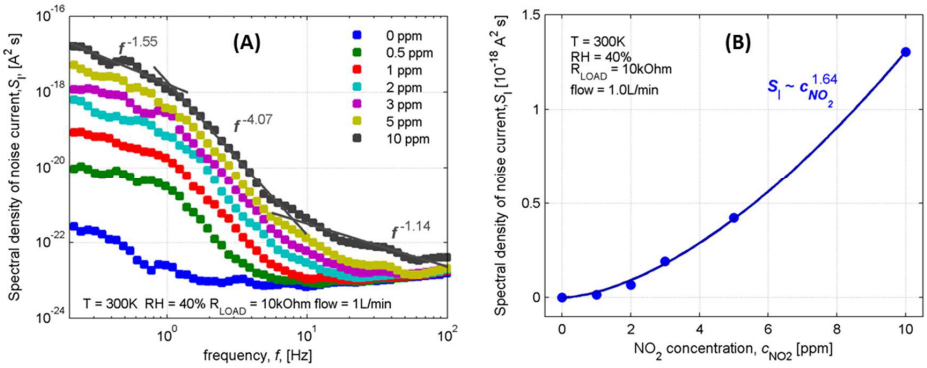

Fig. 6. A laboratory sample: a) the spectral density of current noise measured by the amperometric sensor for NO_2 concentrations from 0 to 10 ppm; b) the spectral density of current noise as a function of NO_2 concentration.

5.1. Effect of non-zero NO_2 concentration on current fluctuations

Figures 6a, 7a and 8a present the spectral densities of current noise in dependence on NO_2 concentrations for a laboratory sample, ceramic Pt/SPE/C samples and a fully printed sample, respectively. The first look revealed that the spectral densities of current fluctuations for all three types show the same shape of spectra for a particular concentration. As the concentration increases, the power spectra of current fluctuations evolve in shape, and also raise their levels in certain frequency ranges. Every spectrum can be divided into three frequency bands whose cut-off frequencies slightly differ according to the type of sample. As the concentration increases to a specific concentration of the detected matter, the spectral densities of current fluctuations show a significant diffusion noise component (indicated by slope –1.5) below 2 Hz for the laboratory samples. In the case of fully printed samples and Pt/SPE/C samples, the power spectra show a significant $1/f$ noise component below 1 Hz. This noise component is also significant for frequencies higher than 10 Hz and also for higher concentrations in the case of fully printed and laboratory samples. As the concentration decreases to zero, desorption processes prevail at the working electrode and the current fluctuations decrease to a level introduced by the thermal and apparatus noise. The bands of spectral densities between the cut-off frequencies show significant components f^{α} with a slope α ranging from –5.5 to –4. This effect might be explained by the presence of time constants (RC constants) in the sensor structure, which result in filtering the $1/f$ noise. These RC constants might be estimated by fitting the equivalent electrical circuit of the sensor [33]. A similar problem was considered for the electrochemical noise [38] as the most probable explanation of this effect. We assume that the phenomenon might be associated with adsorption processes at the electrode/electrolyte interface, especially with adsorption times [39]. The presented experimental results are the object of further studies.

To evaluate the dependence of spectral density of current fluctuations on NO_2 concentration, we focus on spectra in the frequency range below 1 Hz for each type. Figs. 6b, 7b and 8b illustrate an increase of spectral densities by a power of 1.5 to 1.75 as the gas concentration

Metrol. Meas. Syst., Vol. 23 (2016), No. 4, pp. 531–543.

increases. The current flowing through a particular sensor depends linearly on NO_2 concentration of up to 10 ppm according to the used technology [6].

The cut-off frequencies reflect the parameters of adsorbed gas, such as the mass of adsorbed molecules, the effective area of molecules, the average residence time of the molecule on the active surface of the sensor, adsorption times, etc. Thus, the cut-off frequency in the spectrum of density fluctuations measured with a particular sensor is characteristic for the detected gas. We suppose that the relation between the cut-off frequency and a particular gas molecule suggests a possibility for the construction of an artificial nose. Another question is the amplitude of noise and, therefore, sensor sensitivity, however this topic is out of the scope of this paper.

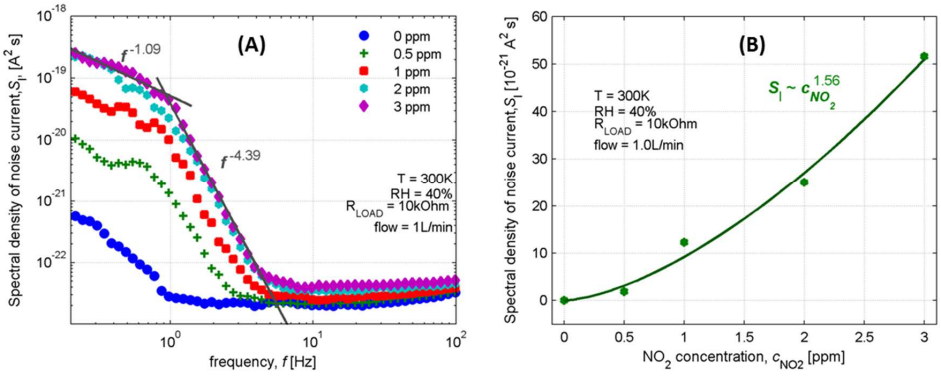

Fig. 7. A ceramic Pt/SPE/C sample: a) the spectral density of current noise measured by the amperometric sensor for NO_2 concentrations from 0 to 10 ppm; b) The spectral density of current noise as a function of NO_2 concentration.

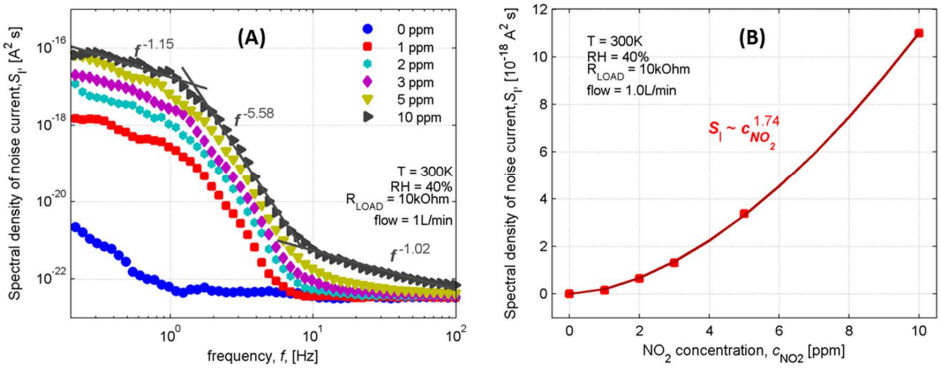

Fig. 8. A PET C/SPE/C sample: a) the spectral density of current noise measured by the amperometric sensor for NO_2 concentrations from 0 to 10 ppm; b) The spectral density of current noise as a function of NO_2 concentration.

5.2. Effect of different fabrication processes on signal-to-noise ratio

As mentioned above, the working electrode/solid polymer electrolyte interface plays a key role in a sensor's performance. To illustrate the influence of WE area on the noise level, WE areas: 4.1 mm^2, 11.4mm^2 and 24.0 mm^2, of three laboratory sample types were examined for NO_2 concentrations from 0 ppm to 15 ppm. Fig. 9a presents that the current response to 1 ppm NO_2 concertation increases with enlargement of WE area. However, the response

stability simultaneously worsens, as described also elsewhere [8, 40]. The spectral density of current fluctuations increases with the area of working electrode, see Fig. 9b.

To illustrate the influence of different technology procedures, the signal-to-noise ratio was examined for three types of samples. The *signal-to-noise ratio* (SNR) was calculated according to the following formula for non-zero mean signals:

$$SNR = 20 \log \frac{\mu}{\sigma}, \tag{1}$$

where μ is the mean value of current flowing through the sensor (in our case – the measured DC current) and σ is the standard deviation, calculated from the corresponding signal acquired during noise measurement. Each type of sensor is different by overall dimension or at least by the area of working electrode, and its way of fabrication. The sizes of WE are: laboratory samples – 4.1 mm^2, ceramic Pt/SPE/C sensor – 11 mm^2, PET C/SPE/C – 18 mm^2. Fig. 10 presents the dependence of *signal-to-noise ratio* (SNR) on NO_2 concentrations. The second type, ceramic Pt/SPE/C sensor, shows the best SNR for low concentration of up to 3 ppm, while fully printed sensors and a laboratory sample with a small area of WE show the best performance for the concentration of up to 10 ppm.

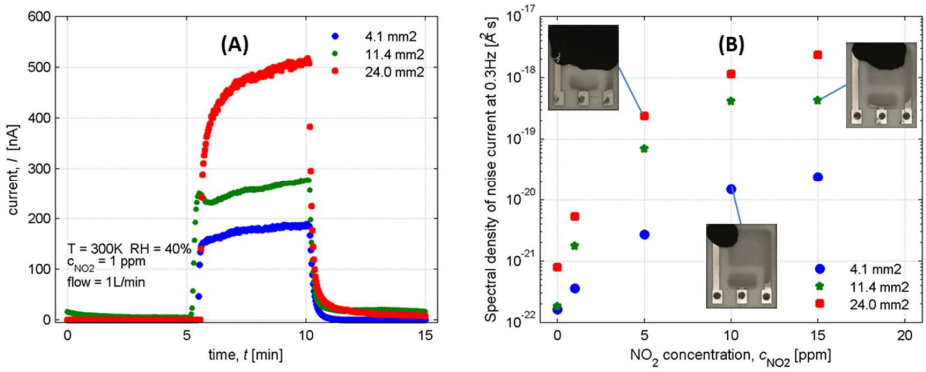

Fig. 9. Laboratory samples with different WE areas: a) the current response to 1 ppm NO2 concentration; b) the spectral density of current noise at 0.3Hz.

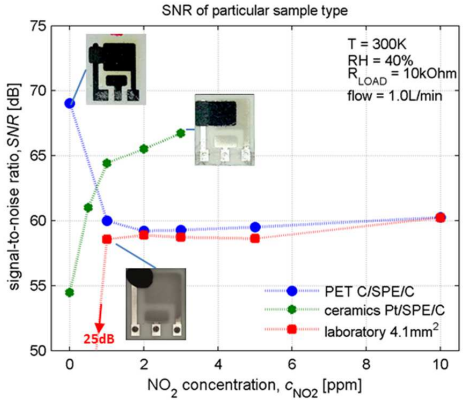

Fig. 10 SNR of a particular sample type.

Metrol. Meas. Syst., Vol. 23 (2016), No. 4, pp. 531–543.

6. Conclusion

The experimental study dealt with current fluctuations in amperometric NO_2 sensors constructed with three fabrication processes: (i) the lift-off and drop-casting technology, (ii) the screen printing technology on a ceramic substrate and (iii) the screen printing on a flexible substrate. The sensors were exposed to a range of NO_2 concentrations from 0 ppm to 10 ppm except for ceramic Pt/SPE/C samples, which were limited to concentrations of up to 3 ppm. The samples were compared from the points of view of the shape and level of spectral density of current fluctuations, dependence of noise spectral densities on NO_2 concentration and signal-to-noise ratios. The spectral density of current fluctuations evolved with changing NO_2 concentration. The level of noise spectral density increases by a power of 1.5 to 1.75 as the gas concentration increases. Comparison of noise figures shows that fully printed samples exhibit a higher level of current fluctuation than laboratory samples and ceramic Pt/SPE/C samples. Nevertheless, the fully printed sensors show stable responses (high signal-to-noise ratio) for the concentration of up to 10 ppm in comparison with other types. The shape of observed noise spectral densities shows two cut-off frequencies. We suppose that the relation between the cut-off frequencies and a particular gas molecule could make possible the construction of an artificial nose.

Acknowledgement

Research described in this paper was financed by the National Sustainability Program under grant LO1401. In the research, the SIX Center infrastructure was used.

References

[1] Xiong, L., Compton, R.G. (2014). Amperometric Gas detection: *A Review, Int. J. Electrochem. Sci*., 9, 7152–81.

[2] Janata, J. (2009). *Principles of Chemical Sensors*. Boston, MA: Springer US.

[3] Stetter, J.R., Li, J. (2008). Amperometric gas sensors a review. *Chem. Rev*., 108, 352–66.

[4] Buzzeo, M.C., Hardacre, C., Compton, R.G. (2004) Use of Room Temperature Ionic Liquids in Gas Sensor. *Design Anal. Chem*., 76, 4583–8.

[5] Silvester, D. S. (2011). Recent advances in the use of ionic liquids for electrochemical sensing. *Analyst*, 136, 4871–82.

[6] Kuberský, P., Sedlák, P., Hamáček, A., Nešpůrek, S., Kuparowitz, T., Šikulam J., Majzner, J., Sedlaková, V., Grmela, L., Syrový, T. (2015). Quantitative fluctuation-enhanced sensing in amperometric NO2 sensors. *Chem. Phys*., 456, 111–7.

[7] Toniolo, R., Dossi, N., Pizzariello, A., Doherty, A.P., Bontempelli, G. (2012). *A Membrane Free Amperometric Gas Sensor Based on Room Temperature Ionic Liquids for the Selective Monitoring of NOx Electroanalysis*. 24, 865–71.

[8] Kuberský, P., Hamáček, A., Nešpůrek, S., Soukup, R., Vik, R. (2013). Effect of the geometry of a working electrode on the behavior of a planar amperometric NO2 sensor based on solid polymer electrolyte. *Sens. Actuators B Chem*., 187, 546–52.

[9] Kuberský, P., Syrový, T., Hamáček, A., Nešpůrek, S., Syrová, L. (2015). Towards a fully printed electrochemical NO2 sensor on a flexible substrate using ionic liquid based polymer electrolyte. *Sens. Actuators B Chem*., 209, 1084–90.

[10] Armand, M., Endres, F., MacFarlane, D.R., Ohno, H., Scrosati, B. (2009). Ionic-liquid materials for the electrochemical challenges of the future. *Nat. Mater*., 8, 621–9.

[11] Rogers, E.I., O'Mahony, A.M., Aldous, L., Compton, R.G. (2010). Amperometric Gas Detection Using Room Temperature Ionic Liquid Solvents. *ECS Trans*., 33, 473–502.

[12] Singh, P.S., Chan, H.S.M., Kang, S., Lemay, S.G. (2011). Stochastic Amperometric Fluctuations as a Probe for Dynamic Adsorption in Nanofluidic. *Electrochemical Systems J. Am. Chem. Soc*., 133, 18289–95.

[13] Rehman, A., Zeng, X. (2012). Ionic liquids as green solvents and electrolytes for robust chemical sensor development. *Acc. Chem. Res*., 45, 1667–77.

[14] Vandamme, L.K.J. (1994). Noise as a diagnostic tool for quality and reliability of electronic devices. *Electron Devices IEEE Trans. On*, 41, 2176–87.

[15] Sedlakova, V., Majzner, J., Sedlak, P., Kopecky, M., Sikula, J., Zarnik, M.S., Belavic, D., Hrovat, M. (2012). Evaluation of piezoresistive ceramic pressure sensors using noise measurements. *Inf. MIDEM*, 42, 109–14.

[16] Zarnik, M.S., Sedlakova, V., Belavic, D., Sikula, J., Majzner, J., Sedlak, P. (2013). Estimation of the long-term stability of piezoresistive LTCC pressure sensors by means of low-frequency noise measurements. *Sens. Actuators Phys*., 199, 334–43.

[17] Santo Zarnik, M., Belavic, D., Sedlakova, V., Sikula, J., Kopecky, M., Sedlak, P., Majzner, J. (2013) Comparison of the Intrinsic Characteristics of LTCC and Silicon Pressure Sensors by Means of 1/*f* Noise. *Measurements Radioengineering*, 22, 227–32.

[18] Contaret, T., Seguin, J.L., Aguir, K., Menini, P. (2013). Adsorption-desorption noise as a selective detection tool for metal-oxide gas microsensors. *22nd International Conference on Noise and Fluctuations*, 1–4.

[19] Schmera, G., Kish, L.B., (2002). Fluctuation-enhanced gas sensing by surface acoustic wave devices. *Fluct. Noise Lett*., 02, L117–23.

[20] Kish, L.B., Li, Y., Solis, J.L., Marlow, W.H., Vajtai, R., Granqvist, C.G., Lantto, V., Smulko, J.M., Schmera, G. (2005). Detecting harmful gases using fluctuation-enhanced sensing with Taguchi sensors. *IEEE Sens. J*., 5, 671–6.

[21] Ayhan, B., Kwan, C., Zhou, J., Kish, L.B., Benkstein, K.D., Rogers, P.H., Semancik, S. (2013). Fluctuation enhanced sensing (FES) with a nanostructured, semiconducting metal oxide film for gas detection and classification. *Sens. Actuators B Chem*., 188, 651–60.

[22] Macku, R., Smulko, J., Koktavy, P., Trawka, M., Sedlak, P. (2015). Analytical fluctuation enhanced sensing by resistive gas sensors. *Sens. Actuators B Chem*., 213, 390–6.

[23] Smulko, J.M., Ederth, J., Li, Y., Kish, L.B., Kennedy, M.K., Kruis, F.E. (2005). Gas sensing by thermoelectric voltage fluctuations in SnO2 nanoparticle films. *Sens. Actuators B Chem*., 106, 708–12.

[24] Contaret, T., Seguin, J., Aguir, K. (2011). Physical-based characterization of low frequency responses in metal-oxide gas sensors 2011. *IEEE Sensors 2011 IEEE Sensors*. 141–4.

[25] Sedlak, P., Sikula, J., Majzner, J., Vrnata, M., Fitl, P., Kopecky, D., Vyslouzil, F., Handel, P.H. (2012) Adsorption-desorption noise in QCM gas sensors. *Sens. Actuators B Chem*., 166–167, 264–8.

[26] Djurić, Z., Jakšić, O., Randjelović, D. (2002). Adsorption-desorption noise in micromechanical resonant structures. *Sens. Actuators Phys*., 96, 244–51.

[27] Ahmadi, M.M., Jullien, G.A. (2009). Current-Mirror-Based Potentiostats for Three-Electrode Amperometric. *Electrochemical Sensors IEEE Trans. Circuits Syst. Regul. Pap*., 56, 1339–48.

[28] Bronzino, J.D. (1999). *Biomedical Engineering Handbook*. CRC Press.

[29] Prasek, J., Trnkova, L., Gablech, I., Businova, P., Drbohlavova, J., Chomoucka, J., Adam, V., Kizek, R., Hubalek, J. (2012). Optimization of planar three-electrode systems for redox system detection. *Int. J. Electrochem. Sci*., 7, 1785–801.

[30] Sedlak, P., Sikula, J., Sedlakova, V., Chvatal, M., Majzner, J., Vondra, M., Kubersky, P., Nespurek, S., Hamacek, A. (2013). Noise in amperometric NO2 sensor. *22nd International Conference on Noise and Fluctuations (ICNF) 2013 22nd International Conference on Noise and Fluctuations (ICNF)*, 1–4.

[31] Sedlak, P., Kubersky, P., Nespurek, S., Majzner, J., Macku, R., Skarvada, P., Sedlakova, V., Hamacek, A., Sikula, J. (2015). Investigation of adsorption-desorption phenomenon by using current fluctuations of amperometric NO2 gas sensor. *23nd International Conference on Noise and Fluctuations ICNF. 22nd International Conference on Noise and Fluctuations ICNF*, Xian, China, *IEEE*, 1–4.

[32] Kuberský, P., Altšmíd, J., Hamáček, A., Nešpůrek, S., Zmeškal, O. (2015). An Electrochemical NO2 Sensor Based on Ionic Liquid. *Influence of the Morphology of the Polymer Electrolyte on Sensor Sensitivity Sensors*, 15(11), 28421–28434.

Metrol. Meas. Syst., Vol. 23 (2016), No. 4, pp. 531–543.

[33] Hassibi, A., Navid, R., Dutton, R.W., Lee, T.H. (2004). Comprehensive study of noise processes in electrode electrolyte interfaces. *J. Appl. Phys*., 96, 1074–82.

[34] Kuo, C.K., Brophy, J.J. (1988). *A Review of Noise Studies in Superionic Electrolytes*. DTIC Document.

[35] Punter, J., Colomer-Farrarons, J., Ll, P. (2013). *Bioelectronics for Amperometric Biosensors State of the Art in Biosensors – General Aspects*. Rinken, T. (ed). InTech.

[36] Sohn, K.S., Oh, S.J., Kim, E.J., Gim, J.M., Kim, N.S., Kim, Y.S., Kim, J.W. (2013) A Unified Potentiostat for Electrochemical Glucose Sensors. *Trans. Electr. Electron. Mater*., 14, 273–7.

[37] Sedlakova, V., Sikula, J., Chvatal, M., Pavelka, J., Tacano, M., Toita, M. (2012). Noise in Submicron Metal-Oxide-Semiconductor Field Effect Transistors: Lateral Electron Density Distribution and Active Trap Position. *Jpn. J. Appl. Phys*., 51, 024105.

[38] Kätelhön, E., Krause, K.J., Mathwig, K., Lemay, S.G., Wolfrum, B. (2014). Noise Phenomena Caused by Reversible Adsorption in Nanoscale Electrochemical Devices ACS Nano, 8, 4924–30.

[39] Smulko, J., Darowicki, K., Wysocki, P. (1998). Digital measurement system for electrochemical noise. *Polish Journal of Chemistry*, 72(7), 1237–1241.

[40] Nádherná, M., Opekar, F., Reiter, J., Štulík, K. (2012). A planar, solid-state amperometric sensor for nitrogen dioxide, employing an ionic liquid electrolyte contained in a polymeric matrix. *Sens. Actuators B Chem*., 161, 811–7.